AAPS PharmSciTech (2026) 27:166
https://doi.org/10.1208/s12249-026-03330-9

RESEARCH ARTICLE

Artificial Intelligence-Guided Optimization of Hyaluronic Acid-Coated Liposomal Linagliptin for Targeted Management of Polycystic Ovary Syndrome

Marwa H. S. Dawoud[1] · Aml H. Zaghloul[2] · Karen S. Zakhari[2] · Mai I. Mahmoud[2] · Zeinab M. Elnagdy[2] · Nyera H. El-Shafei[3] · Mai A. Zaafan[3]

Received: 26 November 2025 / Accepted: 30 December 2025

Abstract

Linagliptin, a DPP-4 inhibitor commonly used in the management of diabetes mellitus, has shown potential activity in polycystic ovary syndrome (PCOS). Linagliptin's therapeutic effectiveness is limited by its poor membrane permeability and low oral bioavailability. This study aimed to formulate hyaluronic acid-coated liposomal linagliptin optimized through I-optimal design and AI-based entrapment efficiency (EE%) prediction. The effects of hyaluronic acid and drug concentrations on particle size (PS), polydispersity index (PDI), zeta potential (ZP), and EE% were systematically evaluated to develop an optimized delivery system for PCOS management. The optimized formulation (O_1) demonstrated a PS of 152.5 nm, PDI of 0.373, ZP of –19.92 mV, and an EE% of 89.43%. The integrated AI-based predictive model achieved 89.8% accuracy, confirming its reliability for rational formulation design. *In-vitro* dissolution studies revealed a sustained drug release over 72 h from O_1, in contrast to complete release within 3 h from unformulated linagliptin. In the PCOS-induced rat model, treatment with both unformulated linagliptin and O_1 significantly improved insulin sensitivity and normalized lipid profiles. Notably, O_1 markedly restored ovarian redox balance through modulation of the Keap1/Nrf2 pathway, indicating a mechanistic basis for the amelioration of PCOS-associated oxidative stress and metabolic dysfunction. Overall, the optimized HA-coated liposomal formulation demonstrated superior therapeutic efficacy and bioavailability compared to unformulated linagliptin, supporting its potential as a targeted repurposed nanocarrier-based therapy for PCOS management, where AI and response surface design are efficient tools for accelerating pharmaceutical formulation development and predicting formulation performance.

Keywords Drug repurposing · Insulin sensitivity · Machine learning · Surface-coated liposomes · Targeted drug delivery

Introduction

Polycystic ovary syndrome (PCOS), is one of the most prevalent endocrine disorders, affecting up to 10% of women of reproductive age worldwide. It is characterized by hyperandrogenism, ovulatory dysfunction, and polycystic ovarian morphology [1]. The etiology of PCOS remains multifactorial, including complex interactions between genetic, hormonal, metabolic, and environmental factors [2]. Clinically, PCOS represents the leading cause of anovulatory infertility, accounting for approximately 90–95% of women seeking fertility treatment [3, 4]. The condition is further defined by the presence of multiple small follicular cysts measuring 2–9 mm within the ovaries, with the diagnosis typically confirmed when twelve or more such follicles are observed [5]. Insulin resistance and compensatory hyperinsulinemia are key features of PCOS pathophysiology, contributing to both its reproductive and metabolic manifestations [6, 7]. Thus, therapeutic approaches often target insulin resistance, with an increasing interest in repurposing anti-diabetic drugs for the management of PCOS [8].

Linagliptin is a dipeptidyl peptidase-4 (DPP-4) inhibitor, that has been approved for the treatment of diabetes miletus Type 2 and has now been recognized as a potential

✉ Marwa H. S. Dawoud
mdawoud@msa.edu.eg; marwahamdysayed@gmail.com

[1] Department of Pharmaceutics, Faculty of Pharmacy, October University for Modern Sciences and Arts, Giza, Egypt

[2] Faculty of Pharmacy, October University for Modern Sciences and Arts, Giza, Egypt

[3] Department of Pharmacology, Faculty of Pharmacy, October University for Modern Sciences and Arts, Giza, Egypt

Published online: 02 April 2026

medication for PCOS because it can modulate metabolic pathways implicated in the syndrome [9]. Linagliptin exerts its action through the inhibition of DPP-4, increasing the levels of incretin hormones like GLP-1 [10], enhancing insulin secretion, and thereby improving glycemic control [9]. In PCOS models, linagliptin has demonstrated promising results by improving insulin sensitivity, reducing systemic inflammation, and modulating androgen levels [11, 12].

Despite its therapeutic potential, linagliptin suffers from poor aqueous solubility, leading to its low oral bioavailability and limited clinical efficacy in non-diabetic indications such as PCOS [13, 14].

Several studies tried to formulate linagliptin to enhance its bioavailability. Linagliptin was formulated as solid dispersions/fast-dissolving systems, polymer carriers (PEG, Soluplus, Kolliphor etc.) to increase apparent solubility and dissolution rate [15]. However, physical instability and recrystallization over time is a common drawback with solid dispersions [16]. Moreover, several nanoparticles-based systems were used as lipid-based systems, which increase solubilization in GI fluids and sometimes enhance lymphatic uptake or inhibit P-gp [13, 14, 17, 18].

Furthermore, polymeric nanoparticles offered as a sustained release, improved apparent bioavailability and changed PK profile of linagliptin [17]. However, these systems are widely known for their burst release, and high degree of complexity [19].

Liposomes is one of the most widely used carriers due to its many advantages such as their biocompatibility, ability to encapsulate both hydrophilic and lipophilic drugs, and potential for controlled release [20–22]. However, conventional liposomes face challenges such as low physical stability, rapid clearance, and limited target specificity [23]. To address these limitations, surface functionalization techniques have been developed. Among them, coating liposomes with hyaluronic acid (HA) has shown considerable promise [24, 25]. HA exhibits high affinity for CD44 receptors, which are overexpressed in ovarian tissues affected by PCOS, enabling targeted drug delivery [26–28].

To further enhance the efficiency of formulation development, artificial intelligence (AI) tools have recently been incorporated in pharmaceutical research [29]. AI models can predict key formulation parameters such as encapsulation efficiency (EE%), thereby reducing experimental workload, minimizing resource consumption, and accelerating optimization [30, 31].

This work uniquely integrates AI-based entrapment efficiency prediction, response surface experimental design, and hyaluronic acid–coated liposomal formulation for the repurposing of linagliptin in targeted PCOS management. To the best of our knowledge, this is the first study to combine these elements within a single formulation-driven and pharmacodynamically validated framework.

The aim of the current study is to build an AI model capable of predicting the EE% of linagliptin-loaded liposomes, and to optimize HA-coated liposomes for effective delivery of linagliptin to be repurposed and targeted to manage PCOS.

Materials and Methods

Materials

Daclatasvir dihydrochloride was supplied as a gift from Marcyrl Pharmaceutical Industries (Cairo, Egypt). Rosuvastatin calcium was supplied as a generous gift from Global Napi Pharmaceutical Company (Cairo, Egypt), while linagliptin was supplied from EVA Pharmaceutical Company, (Cairo, Egypt). Silymarin was supplied as a kind gift from Sedico Company, (Cairo, Egypt). Hyaluronic acid was purchased from CISME, Italy. Lecithin, soybean (90% purity) was procured form Alfa Aeser (ThermoFisher (Kandal), Germany). Cholesterol (≥ 99% purity) was purchased from Merck KGaA, Darmstadt, Germany). Methanol was purchased from Merck, Germany. Methylene chloride, disodium hydrogen phosphate, and hydrochloric acid were purchased from EL mohandes company for modern chemicals, Egypt.

Methods

AI Models Building

Data Collection A pharmaceutical dataset comprising 57 liposome-encapsulated drugs was compiled from various research studies retrieved from the Web of Science (WoS) database, resulting in a total of 418 data entries. The primary input factors found to significantly affect the liposomal entrapment efficiency included XLogP3, molecular weight (Da), number of rotatable bonds, hydrogen bond donors and acceptors, and topological polar surface area, reflecting the drugs' physicochemical characteristics. Additionally, formulation-related variables such as drug quantity, lipid type, lipid additives, lipid amount, cholesterol content, and liposomal surface charge were considered. Furthermore, process-related factors included preparation method, hydration medium, preparation temperature, sonication time and mode, number of extrusion cycles, suction time, hydration duration, organic solvent type, and the organic-to-aqueous solvent ratio. The target variable for the built regression model was the percentage entrapment efficiency of encapsulated drug (EE%).

Only experimentally validated formulation data obtained under controlled and reproducible conditions were included.

Table 1 Hyperparameters Search Space for AI Models

Model	Hyperparameter	Values
SVR	Cost (C)	3
	Regression loss epsilon (Ɛ)	3.5
	kernel	Polynomial
	Iteration limit	300
LR	Regularization	None
DT	Minimum number of instances in leaves	2
	Stop when majority reaches	95%
RF	Number of attributes considered at each split	1
	Replicable training	Yes
	Number of trees	6
Adaboost	Learning rate	0.4
	Fixed seed for random generator	3
	Loss (regression)	Exponential
	Number of estimators	66
GB	Learning rate	0.046
	Number of trees	145
	Replicable Training	Yes
	Lambda	0.5
	Growth control	5
Neural Network	Neurons in hidden layers	140
	Activation function	Logistic
	Solver (optimization)	L-BFGS-B
	Regularization (α)	0.7
	Maximum number of iterations	360

Data Pre-processing To ensure data quality, and enhance the model performance, the dataset was systematically pre-processed through a series of structured steps. Key predictive features were carefully selected to enhance model performance, while categorical variables were transformed using one-hot encoding method to ensure compatibility with regression algorithms. Since most machine learning algorithms require numerical inputs, encoding categorical data to numerical data becomes important. Proper encoding ensures that models can interpret categorical variables effectively, leading to improved predictive accuracy and reduced bias [32]. Incomplete or inconsistent records were removed to preserve data quality and prevent bias, and outliers were excluded. Prior to full preprocessing, the dataset was normalized to a range of [−1, 1] to standardize the input features. Following preprocessing, multiple regression models were developed; namely Support Vector Regressor (SVR), Linear Regression (LR), Decision Tree (DT), Random Forest (RF), AdaBoost, Gradient Boosting (GB), and Neural Network, and their predictive performance was thoroughly assessed using standard statistical metrics, including the coefficient of determination (R^2), mean absolute error (MAE), and root mean square error (RMSE) [33].

Data Splitting Strategy A strategic data splitting approach was employed to enhance model generalizability and prevent overfitting. The dataset was divided into training dataset (70%), validation dataset (15%), and testing (15%) dataset. Hyperparameter tuning was performed using the validation set to optimize model architecture and performance. Final model assessment was carried out on the test set, ensuring unbiased evaluation and robust predictive capability [34].

Model Building EE% was designated as the target variable for prediction. An initial comparative analysis was conducted across seven machine learning algorithms, namely; Support Vector Regressor (SVR), Linear Regression (LR), Decision Tree (DT), Random Forest (RF), AdaBoost, Gradient Boosting (GB), and Neural Network, which were implemented using Orange Data Mining Software® (version 3.38.1). Following model selection, extensive hyperparameter optimization was performed employing 20-fold cross-validation to ensure robustness and generalizability. The defined hyperparameter search space is as detailed in Table 1. To assess the validity and predictive accuracy of the developed model, experimental preparation of four distinct liposomal formulations was conducted. Each formulation encapsulated a different drug, specifically daclatasvir dihydrochloride, rosuvastatin calcium, linagliptin, and silymarin.

Table 2 I-Optimal Design Formulation and Characterization Tests Results, Together with the Optimized Formula as Suggested, Along with the Observed and the Expected Results

Formula code	X_1: HA Coating %	X_2: Drug Concentration (mg/mL)	Y_1: Particle Size (PS) (nm)	Y_2: Polydispersity Index (PDI)	Y_3: Zeta Potential (ZP) (mV)	Y_4: Entrapment Efficiency (EE%)
F_1	0	6	137.6 ± 23.1	0.302 ± 0.03	−19.8 ± 0.3	88.0 ± 4.6
F_2	5	2	232.8 ± 15.0	0.439 ± 0.02	−36.6 ± 0.6	88.6 ± 5.1
F_3	5	6	134.4 ± 11.2	0.372 ± 0.05	−22.2 ± 0.3	88.9 ± 7.3
F_4	0	2	128.8 ± 17.7	0.307 ± 0.07	−31.6 ± 0.4	76.7 ± 2.8
F_5	0	6	135.2 ± 5.4	0.348 ± 0.02	−17.5 ± 0.8	86.0 ± 4.7
F_6	0	2	127.6 ± 10.7	0.338 ± 0.10	−32.7 ± 1.0	75.8 ± 2.8
F_7	5	6	137.0 ± 2.9	0.398 ± 0.02	−23.5 ± 1.6	89.9 ± 5.2
F_8	5	2	232.7 ± 18.4	0.450 ± 0.03	−35.4 ± 0.4	86.7 ± 2.8
F_9	1	2	167.7 ± 1.9	0.330 ± 0.04	−28.6 ± 1.7	75.6 ± 3.8
F_{10}	1	6	150.5 ± 4.8	0.365 ± 0.02	−13.2 ± 0.9	85.6 ± 3.9
F_{11}	1	2	159.3 ± 5.7	0.347 ± 0.09	−29.6 ± 0.4	73.6 ± 3.7
F_{12}	1	6	151.3 ± 7.9	0.361 ± 0.10	−12.09 ± 1.4	88.9 ± 2.9
	HA Coating (%)	**Drug Concentration (mg/mL)**	**PS (nm)**	**PDI**	**ZP (mV)**	**EE%**
Expected Result	2.92	6	143.1	0.369	−17.9	87.9
Observed Result			152.5 ± 4.7	0.373 ± 0.07	−19.9 ± 1.67	89.4 ± 5.7
% prediction error*			6.6	1.1	11.3	1.8

* %Prediction error = (Predicted-Observed)/(Predicted) × 100

These drugs were intentionally selected to represent all four Biopharmaceutics Classification System (BCS) classes: daclatasvir dihydrochloride (Class I), rosuvastatin calcium (Class II), linagliptin (Class III), and silymarin (Class IV), respectively. This approach ensured that the model's performance could be evaluated across a diverse range of drug solubility and permeability characteristics.

Preparation of Liposomes

Liposomes were prepared by thin-film hydration method according to Sweed *et al.*, 2024. In brief, a mixture of soya phosphatidylcholine and cholesterol (in a molar ratio of 4:1) was dissolved in methylene chloride, where the drug was either incorporated into this solution to obtain the drug-loaded formulation or omitted to produce the blank formulation. The organic solvent was then removed under reduced pressure using a rotary evaporator (Heidolph 2, Schwabach, Germany) at 40 °C for 30 min, resulting in the formation of a uniform lipid film. This thin film was further hydrated with distilled water to yield the liposomal dispersion; the latter was then sonicated for 5 min to ensure homogeneity and to minimize the vesicle size [22].

For the preparation of hyaluronic acid (HA)-coated liposomes, the respective aqueous HA solution (1% or 3% w/v) was added drop by drop to the liposomal dispersion under constant stirring by a magnetic stirrer (PM010 JOAN Laboratory Hotplate Magnetic Stirrer, Zhejiang, China) for 5 min to facilitate homogeneous adsorption of HA onto the surface of liposomes and thus to enhance stability and biocompatibility [35].

Response Surface Design

An I-Optimal experimental design was employed to systematically investigate the effect of the studied formulation variables on each of the particle size (PS) (Y_1), polydispersity index (PDI) (Y_2), zeta potential (ZP) (Y_3), and entrapment efficiency (EE%) (Y_4). The independent variables explored were the hyaluronic acid (HA) coating percentage (X_1: 0–5%) and the drug concentration (X_2: 2–6 mg/mL) which were based as the lower and upper limits in the current study based on previous studies [36, 37], as summarized in Table 2, resulting in 12 formulae. This design enabled the efficient modeling of complex formulation behavior with minimal experimental runs [38]. Based on the optimized predictive model with maximum desirability, Design-Expert® software version 13.0.5.0 (Stat-Ease Inc., USA) proposed an optimal formulation (O_1), which was subsequently prepared and experimentally validated. The observed results could confirm the model's reliability and the robustness of the design strategy.

Characterization of Liposomes

Determination of Particle size (PS), Zeta Potential (ZP) and Polydispersity Index (PDI)

Dynamic light scattering (DLS)was used for the determination of the particle size and polydispersity index of the nanoparticles, in addition to the zeta potential. Samples were diluted using distilled water, which were then measured using quartz cuvettes at ambient temperature [39].

Determination of Entrapment Efficiency (EE%) and Drug Loading (DL%)

An indirect method was used for the measurement of EE% of liposomes, where liposomes were centrifugated at 15,300 Xg for 30 min at 4˚C using a cool centrifuge (Megafuge 16R, Hanau, Germany). The drug-loaded liposomal vesicles were separated from the free drug, where the free drug was further measured spectrophotometrically, at its predetermined λ_{max}, at 296 nm, to calculate the EE% and the drug loading, directly in the supernatant according to Eqs. 1 and 2, respectively [40].

$$EE\% = \left(1 - \frac{weight\ of\ drug\ in\ the\ supernatant}{weight\ of\ added\ drug}\right) * 100 \quad (1)$$

$$DL\ \% = \left(1 - \frac{weight\ of\ drug\ in\ the\ liposomes}{supernatant\ weight}\right) * 100 \quad (2)$$

In-vitro Release Rate of Linagliptin

Dialysis bag method was used to evaluate the *in-vitro* release rate of linagliptin. Three preparations were tested: standard linagliptin (5 mg pure linagliptin in water), the optimized hyaluronic acid- coated liposomal dispersion of linagliptin (O_1) (containing 5 mg linagliptin) and the liposomal dispersion of linagliptin (O_2), without HA coating (equivalent to 5 mg linagliptin), which were placed in a dialysis bag (Spectrum Medical Inc., Los Angeles, CA, USA, molecular weight cut off 12,000–14,000 Da). The bags were then immersed in 0.1 N HCl at pH 1.2 for the first two hours which was then replaced with Phosphate Buffer Saline (PBS) at pH 6.8 for the remaining of the study in a thermostatically controlled mechanical shaker at 37 ± 0.50°C at 50 rpm for 72 h. Different samples were withdrawn at time intervals 0.25, 0.5,0.75, 1, 2, 3, 4, 5, 6, 24, 48 and 72 h, and replaced with fresh release medium to maintain sink conditions. The goal was to compare the release profiles of linagliptin from the liposomal dispersion and hyaluronic acid coated liposomal dispersion with the unformulated drug [41].

Transmission Electron Microscopy for Morphological Examination

The morphology of the coated liposomes (O_1) was examined using transmission electron microscopy (TEM, JEOL JSM 6360). Sample preparation involved placing a drop of the formulated dispersion onto a copper grid, followed by negative staining with a 10 µL droplet of 2% phosphotungstic acid solution for 10 s. The grid was then air-dried and subsequently observed under the microscope [42].

Stability Study

The stability of the HA-coated liposomal formulation was assessed in accordance with standard evaluation protocols, encompassing both storage conditions and physicochemical parameter monitoring. Samples were stored at 4 °C and 25 °C under a relative humidity of 55–60% for a period of six months. During this time, the formulations were periodically examined for physical appearance, PS, PDI, ZP, and EE%, to evaluate their stability over the storage duration [42].

Investigation of the Effect of Linagliptin Formulation on Experimentally Induced PCOS in rats

Experimental Animals

Female Wistar albino rats (aged 10–12 weeks; initial weight range 150–160 g) were obtained from the Teodor Bilharis Institute, Cairo, Egypt. The animals were housed in plastic cages at the animal facility of MSA University under controlled conditions (temperature 25 ± 3 ◦C and humidity 50%). They were provided with standard pellet chows and allowed *ad libitum* access to water. All procedures involving the animals were performed under a protocol approved by the Ethics Committee of MSA University (Approval No.: PT88/REC88/2025P).

Animal Experimental Design

A total of 24 female rats were allocated into 4 groups at random, using random number generation via the standard = RAND() function in Microsoft Excel, where each group contained 6 animals. Sample size was calculated using G*Power software based on anticipated differences in blood glucose levels, with a statistical power of 80%. The first group was the normal group, and the second group (PCOS-control group) injected with letrozole (1 mg/kg; p.o.) daily for 21 days for induction of polycystic ovarian syndrome (PCOS) [43]. The third group, which was also induced with

PCOS received linagliptin (10 mg/kg, p.o.) for 30 days starting from the day of induction. The last group, was induced with PCOS, were treated with linagliptin formulation (O_1) in the same dose and duration. All injections started on the same day, and induction continued for 21 days. Treatments lasted for 30 days (continued for one week after stopping drug of induction). The dose and route of administration of linagliptin were chosen based on previous literature [44]. At the end of the experiment, rats were terminated by cervical dislocation under ketamine anesthesia. The abdominal cavity was opened, and ovaries were harvested and weighed to be used for histopathological examination and biochemical parameters investigations.

Biochemical Assays

The blood samples were used for assessment of the following parameters including serum levels of insulin using standard ELISA kit (Cat no.: MBS724709), and colorimetric assay kit for glucose (Cat. No.: E-BC-K234-S), total cholesterol (Cat. No.: E-BC-K109-S) and total triglycerides (Cat. No.: E-BC-K238) according to the manufacturer instructions (Elabscience, TX, USA).

Moreover, homeostasis model assessment-insulin resistance (HOMA-IR) was calculated to assess insulin resistance from basal glucose and insulin levels according to Equation 3 [45].

$$HOMA-IR = Fasting\ Insulin\ (\mu IU/mL) \times Fasting\ Glucos\ e\ (mmol/L)\ /\ 22.5 \quad (3)$$

The glucose concentrations were converted from mg/dL to mmol/L using the molecular weight value of glucose 18.018.

The isolated ovaries were used for investigating the levels of nuclear factor erythroid 2-related factor 2 (Nrf2) and its repressor, Kelch-like ECH-associated protein 1 (Keap-1), using standard ELISA kits (Cat. No. MBS012148 and MBS714561, respectively, MyBioSource, San Diego, CA, USA).

Histopathological Examination of the Ovarian Tissue

Ovarian tissues from the different groups were washed and fixed in neutral formalin solution. After being trimmed and processed according to Culling., 2013 [46], tissue sections were cut with a rotatory microtome and stained with H&E stain and examined under light microscope. The Full HD microscopic imaging system (Leica Microsystems GmbH, Germany) with Leica Application software for tissue section analysis was used to collect the data.

Statistical Analysis

Optimization analysis was carried out using Design-Expert software (version 13.0.5.0®, Stat-Ease Inc., Minneapolis, USA). Model performance was evaluated by comparing the multiple correlation coefficient (R^2), as well as the adjusted and predicted R^2 values. Statistical significance was defined at a $p < 0.05$.

Data obtained from the stability, and *in-vivo* pharmacodynamic studies were expressed as mean ± SEM. The Shapiro–Wilk test was used to check the data normality. The Tukey–Kramer multiple comparisons test was used after the one-way ANOVA test to compare the means of the different groups. The significance threshold was established at $p < 0.05$. All statistical analyses were performed using GraphPad Prism version 8 (GraphPad® Software, Inc., USA).

Results and Discussion

AI Models

AI, specifically machine learning models were developed to predict the EE% of the drug within liposomes, using the previously described input variables. A range of algorithms with varying modelling approaches were explored and compared to identify the most effective one for EE% prediction. Following hyperparameter tuning, all regression models were evaluated using coefficient of determination (R^2), MAE, and RMSE, as summarized in Table 3. As can be observed, the Decision Tree Regressor (DT) demonstrated the highest predictive accuracy, achieving the best R^2 along with the lowest MAE and RMSE.

The performance of the selected AI model was further evaluated by comparing the coefficient of determination (R^2) across the training, validation, and test datasets. The AI model exhibited R^2 values of 0.903, 0.790, and 0.898 for the training, validation, and test datasets, respectively, indicating consistent predictive performance across all data partitions. The relatively close agreement between the training and external dataset R^2 values suggests effective model learning without excessive memorization, thereby minimizing the risk of overfitting [47]. Importantly, the comparable validation and test R^2 values demonstrate good generalizability of the model when applied to unseen data [48]. Such performance consistency is considered a hallmark of robust regression models, particularly in pharmaceutical formulation studies where dataset sizes are often limited and experimental variability is unavoidable [49].

Table 3 Evaluation Performance of ML Algorithms, with the Predicted and Expected Results from the Built ML Models

Model		R^2	RMSE	MAE
SVR		0.765	12.997	9.328
LR		−1.261	40.290	27.572
DT		0.898	8.574	4.163
RF		0.840	10.711	7.442
Adaboost		0.830	11.044	6.985
GB		0.878	9.352	6.318
Neural Network		0.761	13.100	8.477
	EE% of Daclatasvir Dihydrochloride	EE% of Rosuvastatin Calcium	EE% of Linagliptin	EE% of Silymarin
Predicted Results	82.50%	79.33%	68.73%	60.20%
Observed Results	90.37%	70.20%	73.77%	66.21%
% Prediction error*	9.50%	11.50%	7.33%	9.98%

*$\%\text{Prediction error} = \frac{\text{Predicted}-\text{Observed}}{\text{Predicted}} \times 100$

The model's performance was further validated experimentally by formulating liposomes with four different drugs and measuring their EE%. The predicted values were then compared to the actual results to calculate the prediction error, thereby confirming the model's reliability as shown in Table 3.

The experimental results demonstrated a high level of agreement with the entrapment efficiency values predicted by the AI-based model for the liposomal formulation. This successful alignment highlights the robust predictive capability of the AI approach and reinforces its value in accurately predicting entrapment efficiency across different drug candidates within optimized liposomal systems.

Preparation of Liposomes

Liposomes prepared by thin film hydration technique are characterized by high encapsulation of poorly-water soluble drugs, and is simple, flexible and scalable process that protects the drug from degradation [50].

HA-coated liposomes enhance the drug encapsulation and have a wide application in targeted delivery. HA coating enhances adhesion and uptake of the liposomes by specific cells and hence is ideal for targeted delivery. Since the overexpression of the CD44 receptors occurs in the ovaries of females with PCOS, the high binding affinity of HA to its receptors provides a strategic approach for increasing the drug targeting specifically to PCOS-affected ovarian tissue by coating the liposomes with HA [4]. Furthermore, the anti-inflammatory and antioxidant properties of HA may be beneficial in addressing inflammation within the ovarian tissues of women with PCOS. By suppressing cytokines, HA can reduce inflammation and provide protection against oxidative stress [51].

Response Surface Optimization using I-Optimal Experimental Design

The results of the prepared formulae in terms of PS, PDI, ZP and EE% are shown in Table 2.

Particle Size Analysis

The particle size was found to be in the range from 127.6 ± 10.7 to 232.8 ± 15.0 nm as can be deduced from Table 2. Effective targeting of ovarian tissue in PCOS requires overcoming biological barriers and ensuring adequate tissue penetration. Although nanoparticles sized between 50–100 nm typically exhibit superior tissue penetration due to their efficient transcellular transport [13], larger particles in the range of 200–250 nm may enhance the bioavailability of linagliptin formulations. This can be attributed to the relationship between particle size, surface coating, and biological interaction. The presence of the HA layer improves mucoadhesion and receptor-mediated interactions with CD44 receptors, which is highly expressed in PCOS [52]. Additionally, the increase in size due to HA coating could enhance the uptake of the nanoparticles by the CD44 receptors in the ovaries of females [4], and it also demonstrates prolonged residence time at the absorption site and reduced systemic clearance, which allows for sustained drug release and improved local drug concentration gradients; as they are less susceptible to rapid renal clearance [53]. Furthermore, the HA coating enhances the stability of the liposomal bilayer and reduces premature drug leakage, maintaining the structural integrity required for efficient delivery [54]. Also, PCOS is associated with chronic low-grade inflammation and changes in vascular permeability, thus larger nanoparticles may benefit from the enhanced permeability and retention (EPR) effect in the altered ovarian

microenvironment, allowing better drug accumulation in the affected tissue [55].

In case of linagliptin, whose oral absorption is limited by efflux and enzymatic degradation [56], the optimized particle size of 200–250 nm ensures a balance between sufficient tissue interaction and extended retention, ultimately contributing to higher bioavailability and improved therapeutic performance.

Further analysis of I-Optimal design (ANOVA) as presented in Table 4, shows a significant 2-factor interaction model. The observed increase in the PS with higher levels of HA coating (X_1) as observed from Equation 4, can be attributed to the deposition of an additional HA layer on the liposomal surface, which increases the overall hydrodynamic diameter. HA, being a high-molecular-weight and hydrophilic polysaccharide, forms a dense, hydrated shell around the liposomes through electrostatic and hydrogen-bonding interactions. This coating not only enlarges the particle size but also enhances colloidal stability by providing steric hindrance and surface charge modification [57]. Conversely, the decrease in the PS with increasing the drug concentration (X_2) may be due to the influence of drug loading on liposomal membrane packing. At higher linagliptin concentrations, drug molecules may integrate within the lipid bilayer, leading to tighter molecular packing and reduced vesicle diameter. Additionally, higher drug content can alter the interfacial tension between the lipid and aqueous phases during formulation, resulting in the formation of smaller, more compact vesicles [58].

The correlation coefficient (R^2) was 0.9974, and the difference between the adjusted R^2 (0.9963) and predicted R^2 (0.9933) values less than 0.2, while the adequate precision was 68.1744, confirming the reliability and validity of the experimental design.

It is worth mentioning that a difference of less than 0.2 between the adjusted R^2 and predicted R^2 values is widely accepted as evidence of adequate model predictability and validation, indicating that the developed model is neither overfitted nor lacking predictive reliability [59–62].

The coefficient of determination (R^2) was employed to assess the overall goodness of fit of the regression model, while the adjusted R^2 was used to account for the number of predictors and reduce the risk of overfitting. In addition, the predicted R^2 was utilized to evaluate the model's predictive performance on unseen data, providing an estimate of its generalizability. The combined use of these metrics enables a more reliable and interpretable assessment of model robustness [59–61, 63].

As can be observed from the 3-D response surface plot (Fig. 1a) showing the interaction effect of the studied factors on the particle size, that increasing the HA coating together with slightly increasing in drug concentration resulted in a significant increase in the PS.

Polydispersity Index Analysis

As shown in Table 2, the PDI values ranged from 0.302 ± 0.03 to 0.450 ± 0.03, indicating a relatively homogeneous particle size distribution within the formulation. A lower PDI reflects a more uniform population of liposomes, which is critical for ensuring consistent drug delivery, enhanced formulation stability, and improved therapeutic efficacy [64].

Further analysis of the I-Optimal design (ANOVA) (Table 4), together with Equation 5, showing a 2-factor interaction model, demonstrated that an increase in HA coating was associated with a significant rise in PDI. This could be due to the formation of a thicker and more heterogeneous surface layer on the liposomes by adding more HA. As HA is adsorbed more onto the lipid bilayer, it physically expands the particle size and creates variability in coating thickness, resulting in a broader size distribution of vesicles. This heterogeneity is often attributed to the nanoscale effect of HA, which forms an additional external layer through physical adsorption, leading to more aggregates or less uniformity across the population [65]. Notably, a significant interaction between X_1 and X_2 was observed, indicating that an optimal balance between these variables enhances liposomal homogeneity.

The correlation coefficient (R^2) was 0.8775, with the difference between the adjusted R^2 (0.8249) and predicted R^2 (0.6456) below 0.2, and an adequate precision of 9.9368, indicates the robustness and validity of the experimental design.

As can be observed from the 3-D response surface plot in Fig. 1b, that increasing the HA coating together with increasing in drug concentration resulted in a significant increase in the PDI.

Zeta Potential Analysis

Zeta potential is a marker for stability, time in circulation, interactions with proteins and permeability and thus biocompatibility [66]. As can be deduced from Table 2, the zeta potential ranged from -12.09 ± 1.4 to -36.6 ± 0.4 mV.

ANOVA as presented in Table 4, shows a linear significant model. As can be deduced from Equation 6, that the increase in HA coating (X_1) resulted in an increase in ZP, while the increase in drug concentration (X_2) leads to decrease in ZP.

The increase in ZP with higher levels of HA coating (X_1) can be explained by the presence of negatively charged carboxyl and hydroxyl groups on the HA chains. As the HA concentration increases, more of these ionizable groups are exposed over the liposomal surface, enhancing the negative surface charge and thus increasing the magnitude of the ZP [28]. This stronger surface charge contributes to an improved

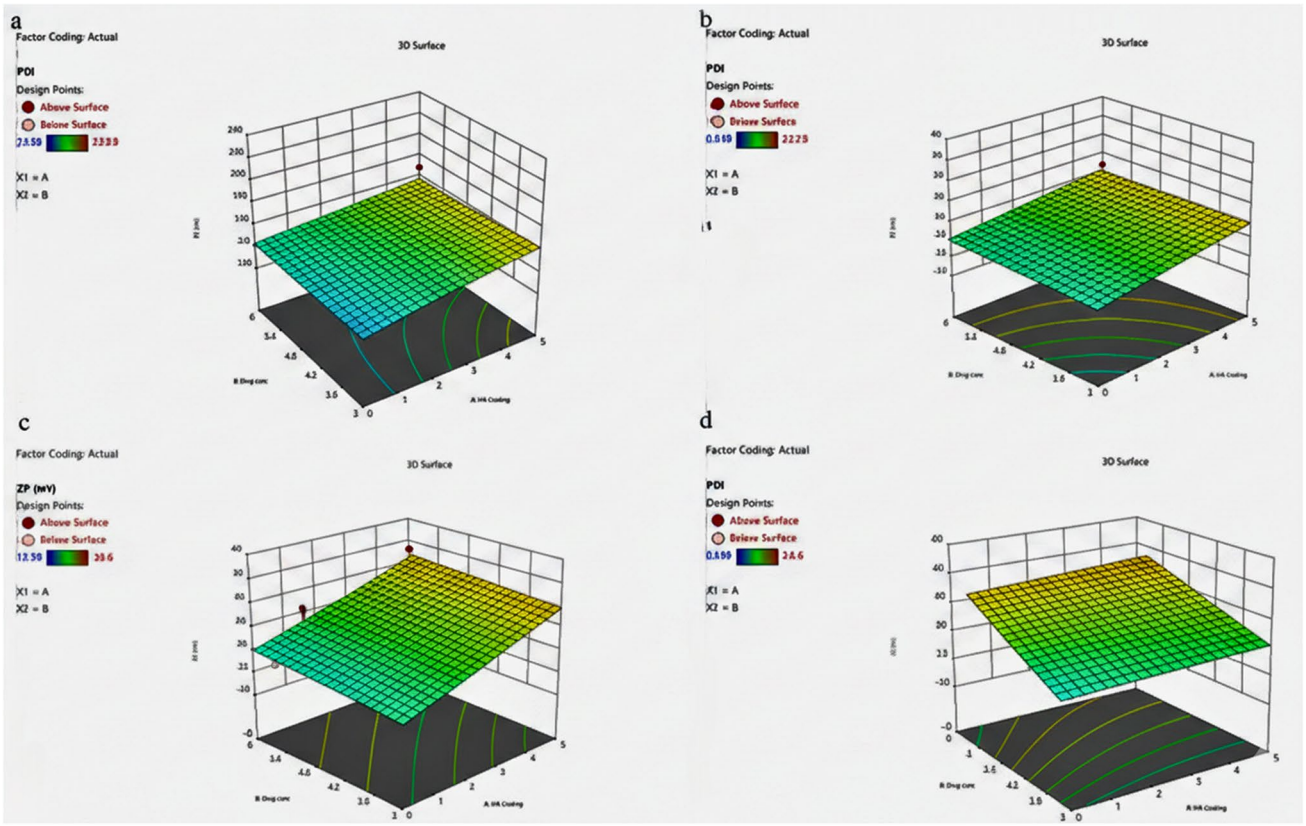

Fig. 1 3D response surface plots showing the effect of the HA% (X1) and the drug amount (X2) on the **a** particle size (PS), **b** polydispersity index (PDI), **c** zeta potential (ZP) and **d** entrapment efficiency (EE%)

electrostatic repulsion between particles, which in turn enhances colloidal stability and reduces the likelihood of aggregation [67]. On the other hand, the observed decrease in ZP with increasing drug concentration (X_2) may be attributed to the interaction of the drug molecules with the lipid bilayer and the HA coating. Linagliptin carries functional groups that can partially neutralize surface charges or mask the ionizable groups of HA, leading to a reduction in overall surface potential [68].

The correlation coefficient was found to be 0.9811 and the difference between the adjusted R^2 (0.9764) and predicted R^2 (0.9576) was less than 0.2 and adequate precision of 31.7301, indicating the validity of the design.

As can be observed from the 3-D response surface plot (Fig. 1c), that increasing the HA coating, together with decreasing the drug concentration causes an increase in ZP.

Entrapment Efficiency Analysis

It can be observed from Table 2 that the EE% of the different liposomal formulations ranged from $73.56 \pm 3.7\%$ to $89.87 \pm 5.2\%$, and the drug loading was found to be $18 \pm 1.67\%$.

Further ANOVA as depicted in Table 4, shows that there is a significant 2-factor interaction model. As can be deduced from Equation 7, that when either HA% or the drug concentration increases the EE% increases. Indeed, concomitant increase in EE% with greater HA coating can be explained by several complementary mechanisms. First, a HA shell forms a physical barrier around the liposome that hinders drug diffusion out of the vesicle, reducing leakage during both preparation and subsequent handling [69]. Second, HA increases the effective viscosity of the microenvironment around vesicles and/or promotes tighter packing of the outer leaflet, both of which slow drug leakage [70]. Third, specific interactions between HA functional groups, for example, hydrogen bonding or ionic interactions, with polar groups of linagliptin, may stabilize drug association with the liposome surface or near-surface regions, thereby effectively increasing apparent entrapment [68]. Finally, HA coating often improves the colloidal stability, due to electrosteric stabilization, thereby reducing the likelihood of fusion or rupture events that release encapsulated drug [71].

Whereas the trend of increasing EE% with increasing the drug amount may simply reflect simple mass-action and partitioning effects: the more linagliptin available in

Table 4 ANOVA of I-Optimal Design

Source	Y_1: *Particle Size*					Y_2: PDI					Y_3: ZP (mV)					Y_4: EE%				
	Sum of Square	df	Mean Square	F value	*p-value*	Sum of Squares	df	Mean Square	F-value	*p-value*	Sum of Squares	df	Mean Square	F-value	*p-value*	Sum of Squares	df	Mean Square	F-value	*p-value*
Block	6.10	1	6.10			0.0009	1	0.0009			114.06	1	114.06			45.77	1	45.77		
Model	15,034.53	3	5011.51	886.82	< 0.0001	0.0200	3	0.0067	16.71	0.0014	651.75	2	325.87	208.17	< 0.0001	368.79	3	122.93	41.72	< 0.0001
X_1	2844.86	1	2844.86	503.41	< 0.0001	0.0126	1	0.0126	31.69	0.0008	32.40	1	32.40	20.70	0.0019	59.57	1	59.57	20.22	0.0028
X_2	5593.36	1	5593.36	989.78	< 0.0001	0.0009	1	0.0009	2.38	0.1669	619.35	1	619.35	395.64	< 0.0001	156.53	1	156.53	53.13	0.0002
X_1X_2	6218.18	1	6218.18	1100.34	< 0.0001	0.0031	1	0.0031	7.74	0.0272						59.62	1	59.62	20.23	0.0028
Residual	39.56	7	5.65			0.0028	7	0.0004			12.52	8	1.57			20.62	7	2.95		
Lack of Fit	0.0729	1	0.0729	0.0111	0.9196	0.0007	1	0.0007	2.02	0.2048	6.59	2	3.30	3.33	0.1062	8.32	1	8.32	4.06	0.0907
Pure Error	39.49	6	6.58			0.0021	6	0.0003			5.93	6	0.9885			12.31	6	2.05		
Cor Total	15,080.19	11				0.0237	11				778.33	11				435.18	11			
Regression equation	$PS = +159.75 + 19.38X_1 - 16.62X_2 - 19.76X_1X_2$ *Equation 4*					$PDI = +0.3714 + 0.0409X_1 - 0.0068X_2 - 0.0139X_1X_2$ *Equation 5*					$ZP = +22.95 + 2.01X_1 - 5.39X_2$ *Equation 6*					$EE\% = +84.96 + 2.80X_1 + 2.78X_2 - 1.93X_1X_2$ *Equation 7*				

solution during the liposome formation process, the greater the proportion of the compound will partition into the forming bilayer or aqueous core before the vesicles close, so more drug is physically entrapped, rather than lost to the external phase [72]. Increasing the drug feed also increases the chemical potential driving encapsulation and can decrease the relative proportion of free drug remaining in the dispersion, until the loading capacity of the bilayer or core is approached [73].

The correlation coefficient (R^2) was found to be 0.9470 and the difference between the adjusted R^2 (0.9470) and the Predicted R^2 (0.8583) was less than 0.2 with an adequate precision of 12.9168, meeting established design-validation thresholds as reported in the literature [72].

3-D response surface plot, representing the interaction between the HA% and the drug concentration on the EE% (Fig. 1d), shows that increasing the HA coating together with increasing in drug concentration resulted in a significant increase in the EE%.

Response Surface Optimization

The optimized formulation (O_1), as proposed by the software, was subsequently prepared and evaluated using the previously described characterization tests. The experimental results were then compared with the model's predicted values to assess the accuracy of the optimization process. Prediction errors were calculated accordingly (Table 1). A high degree of agreement between the predicted and experimental results was observed, which substantiates the strength and reliability of the experimental design.

A nanoparticle system exhibiting a moderate particle size (152.5 nm), narrow size distribution (PDI = 0.373), and a relatively high negative zeta potential (−19.9 mV) suggests a strong potential to evade the reticuloendothelial system (RES) while facilitating enhanced targeted delivery [74]. The optimized formulation (O_1) underwent further characterization to assess its stability and therapeutic efficacy.

In-vitro Release Rate of Linagliptin

The comparison of drug release profiles among standard linagliptin, liposomal linagliptin, and HA-coated liposomal linagliptin demonstrates the substantial impact of carrier systems and surface modifications on drug delivery performance (Fig. 2a). Standard linagliptin showed limited and incomplete release (only 40% release within 3 h, with minimal increase up to 72 h), likely due to its low solubility and the lack of a delivery matrix, which causes release to be dictated primarily by simple diffusion across the dialysis membrane [41].

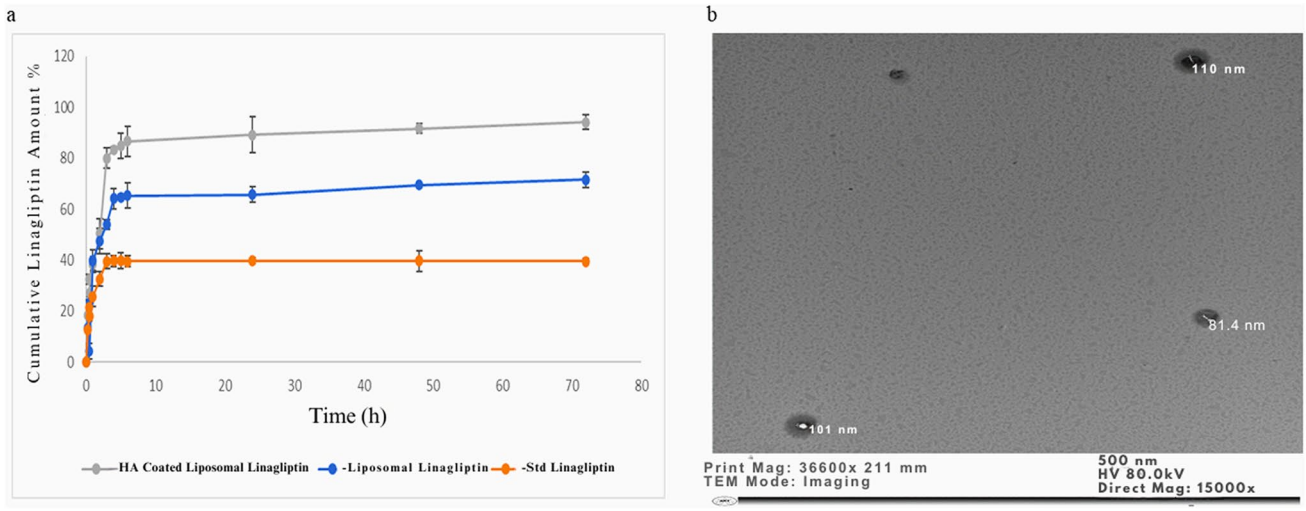

Fig. 2 **a** *In-vitro* release rate of linagliptin from liposomes and HA-coated liposomal formulation in simulated intestinal condition as compared to the standard linagliptin, and **b** Morphological structure as obtained from TEM of the optimized HA-coated liposomal formulation

In contrast, encapsulating linagliptin in liposomes increases the extent and duration of release (approximately 65% release within 4 h, followed by sustained delivery (about 65% at 24 h and 71% at 72 h)), with the lipid bilayer acting as a physical barrier that retards drug diffusion, resulting in a more controlled and sustained profile over 72 h. This aligns with findings from other vesicle-based formulations, where the bilayer structure modulates drug permeability and helps maintain prolonged therapeutic levels [75]. Notably, when liposomes are coated with hyaluronic acid, an even faster initial drug release is observed, followed by enhanced and sustained release at later time points. The HA coating, being hydrophilic and highly dispersible, likely improves the interaction between liposomes and the aqueous medium, resulting in accelerated drug release from the liposomal matrix, reaching 80% of the drug diffusing from the dialysis bag within 3 h, and sustained release thereafter (approximately 89% at 24 h and 94% at 72 h). This synergistic effect highlights HA's dual role: it provides both targeted delivery potential; through interactions with CD44 receptors, and physicochemical enhancement of release kinetics, as reported in similar studies on surface-modified carriers [18]. These modifications may be particularly advantageous when rapid onset and extended maintenance of drug levels are desired, thus supporting further exploration of HA-coated liposomal systems for linagliptin in the management of PCOS.

Morphological Evaluation of HA-coated Liposomes

Morphological examination of the HA-coated liposomes (Fig. 2b), showed vesicles' diameters ranging from 81.4 to 110 nm. The liposome core displayed a lighter appearance and maintained a spherical shape due to the uniform coating of the surrounding black HA shell. Notably, particle sizes determined via DLS were larger than those obtained by TEM, as DLS assesses the hydrodynamic diameters of the nanovesicles, whereas TEM measures the particle diameter in its dried state [41].

Stability Study Analysis

The optimized formulation (O_1) maintained robust stability during refrigerated storage at 4 °C, with no observable physical changes such as precipitation or aggregation over the course of six months. In contrast, at 25˚C, O_1 showed visible aggregation, indicating compromised stability under elevated temperatures. As shown in Table 5, the physicochemical parameters, including PS, PDI, ZP, and EE%, remained relatively stable at 4 °C with no statistically significant changes over 6 months. However, storage at 25°C induced statistically significant variations in PS, PDI, ZP and EE%. These observations underscore the importance of low temperature conditions for long-term preservation of liposomal formulations, consistent with established pharmaceutical guidance for maintaining colloidal stability and drug retention.

It is worth mentioning that although solid lipid nanoparticles (SLNs) and nanostructured lipid carriers (NLCs) offer higher physical stability and simpler scale-up processes compared to conventional liposomes due to their solid lipid core, providing sustained release and potentially enhanced oral bioavailability; however, surface functionalization for specific tissue targeting remains an ongoing challenge [76].

Table 5 Stability Study Results at the 2 Storage Temperatures

	4°C				25°C			
	0 month	1 month	3 months	6 months	0 month	1 month	3 months	6 months
PS (nm)	152.5 ± 4.7	159.9 ± 12.2	161.5 ± 11.5	178.7 ± 12.1	152.5 ± 4.7	179.07 ± 11.7*	209.34 ± 10.4*	321.71 ± 12.6*
PDI	0.373 ± 0.07	0.389 ± 0.08	0.385 ± 0.07	0.401 ± 0.03	0.373 ± 0.07	0.403 ± 0.08	0.423 ± 0.06	0.545 ± 0.03*
ZP (mV)	−19.9 ± 1.67	−18.90 ± 1.6	−17.76 ± 2.6	−16.90 ± 0.8	−19.9 ± 1.67	−16.82 ± 2.4	−14.76 ± 2.7*	−10.62 ± 1.7*
EE%	89.4 ± 5.7	87.78 ± 2.9	86.09 ± 3.7	85.75 ± 4.6	89.4 ± 5.7	84.99 ± 7.9*	69.98 ± 2.6*	57.67 ± 2.2*

*Statistically significant at $p < 0.05$. Results are presented as mean ± SD

Importantly, composite and hybrid strategies (e.g., liposome-hydrogel composites) have been investigated to combine the controlled release of hydrogels with liposomal encapsulation benefits, particularly for localized and sustained delivery in chronic conditions, but often at the cost of increased formulation complexity and regulatory hurdles [77].

The Effect of Linagliptin Formulation on Experimentally Induced PCOS in Rats

The Effect on Serum Glucose, Insulin and Insulin Resistance

The PCOS control group exhibited a significant elevation in the blood glucose levels compared to the normal group ($p < 0.01$), underscoring the hyperglycemic state characteristic of insulin resistance in the PCOS model. Furthermore, there was a significant elevation in serum insulin levels in the PCOS control group compared to the normal group ($p < 0.001$). Treatment with formulated linagliptin (O_1) resulted in a notable reduction in glucose concentrations relative to the PCOS group ($p < 0.05$). These findings highlight the potential of linagliptin, particularly in its formulated form, to ameliorate hyperglycemia and improve glycemic control in the context of PCOS-associated metabolic disturbances. Moreover, treatment with linagliptin significantly attenuated hyperinsulinemia relative to the PCOS group ($p < 0.01$). Linagliptin formulation (O_1) further reduced insulin concentrations, approaching near-normal levels and exhibiting significant improvement over the PCOS ($p < 0.0001$) (Fig. 3a and b).

PCOS control group demonstrated substantial insulin resistance, where PCOS-induced rats showed a marked elevation in HOMA-IR values (mean ≈ 8.66), affirming significant insulin resistance in the model. This reflects the compounded effect of hyperinsulinemia and hyperglycemia, typical of PCOS-related metabolic disruption. This validates the model and aligns with prior studies linking hyperinsulinemia and elevated glucose levels to PCOS pathophysiology. The normal group showed stable glucose-insulin homeostasis, where the baseline HOMA-IR values were low (mean ≈ 1.81), consistent with normal insulin sensitivity. These serve as a reliable benchmark for assessing therapeutic reversal. Treatment with unformulated linagliptin significantly reduced HOMA-IR to a mean of 4.88. This partial normalization suggests beneficial glycemic and insulinemic modulation, likely through DPP-4 inhibition, enhanced GLP-1 activity, and improved insulin sensitivity [44]. The most striking recovery appears in the formulated linagliptin group (O_1) (mean HOMA-IR ≈ 2.44). This suggests a profound enhancement in efficacy possibly due to improved bioavailability that augment glycemic control and insulin responsiveness (Fig. 3C). The HA coating of the liposomal carrier played a pivotal role in enhancing the pharmacological efficiency of linagliptin. HA, a naturally occurring glycosaminoglycan, binds selectively to CD44 receptors, which are overexpressed in inflamed ovarian and hepatic tissues commonly associated with PCOS. This receptor-mediated interaction facilitates site-specific drug delivery, improving local drug accumulation and minimizing systemic exposure [26, 78]. Furthermore, HA provides mucoadhesive and stabilizing properties, protecting the liposomes from enzymatic degradation in the gastrointestinal environment and promoting sustained drug release [26]. The result is an improved pharmacokinetic profile, characterized by enhanced oral bioavailability and prolonged DPP-4 inhibition. Additionally, HA contributes intrinsic anti-inflammatory and antioxidative effects, which may further restore insulin signaling pathways disrupted in PCOS. By mitigating oxidative stress and inflammatory cytokine expression, HA supports the reactivation of downstream insulin receptor substrates, thus complementing the pharmacological action of linagliptin [79]. These combined mechanisms likely explain the pronounced normalization of insulin levels observed with the HA-coated formulation.

While liposomal systems are well-established for enhancing the delivery of poorly bioavailable drugs, various other nanocarrier platforms have been explored and, in some contexts, offer distinct advantages or present different challenges compared to HA-coated liposomes. Liposomes, particularly when surface-modified with targeting ligands such as hyaluronic acid, improve drug solubility, protect the payload from premature degradation, and facilitate targeted uptake via receptor-mediated endocytosis (e.g., CD44) in tissues expressing the cognate receptor, enhancing therapeutic

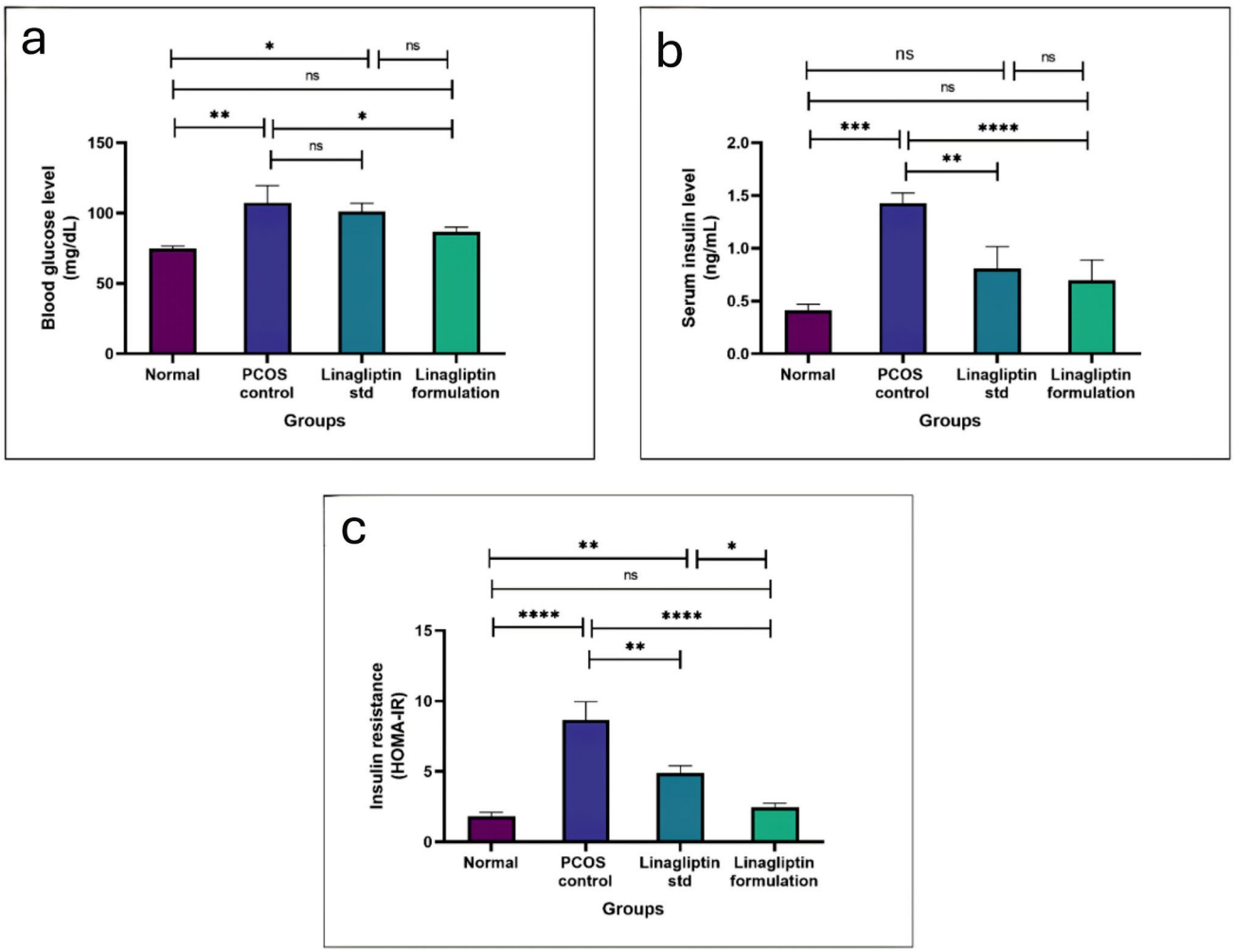

Fig. 3 Effect of linagliptin and its formulation on **a** Serum glucose, **b** Insulin and **c** Insulin Resistance (HOMA-IR) in PCOS-induced Rats. Data are presented as mean ± SEM ($n = 6$). Levels of significance include ns: non-significant, * $p<0.05$, ** $p<0.01$, *** $p<0.001$, ****$p<0.0001$

efficacy while reducing systemic side effects. HA-based nanocarriers have demonstrated increased accumulation in target tissues and improved therapeutic outcomes in cancer models, attributed to active targeting and enhanced cellular internalization relative to non-targeted counterparts [80]. Alternative vesicular systems like niosomes provide enhanced storage stability and may show better shelf-life characteristics than phospholipid liposomes, yet they may be less efficient in passive targeting without surface ligands [76].

The Effect on Serum Total Triglycerides and Cholesterol Levels

The PCOS control group exhibited a significant elevation in triglyceride and cholesterol levels relative to the normal group ($p < 0.0001$), reflecting the dyslipidemic profile associated with PCOS. The observed elevation in serum triglyceride and cholesterol levels in the PCOS control group corroborates the metabolic disturbances commonly associated with PCOS, including insulin resistance and altered lipid metabolism. Both linagliptin-treated groups showed a marked reduction in serum triglycerides and cholesterol compared to the PCOS control. While the linagliptin formulation group (O_1) demonstrated a numerically lower triglyceride level than the linagliptin standard group, without significant difference from the normal group (Fig. 4a and b). Treatment with linagliptin, a DPP-4 inhibitor, significantly ameliorated hypertriglyceridemia and hypercholesterolemia potentially through enhancement of incretin action and downstream modulation of lipid homeostasis. Linagliptin was reported for its potential in lowering total cholesterol and LDL levels in patients with type 2 diabetes [81]. Notably, the linagliptin formulation group showed a trend toward

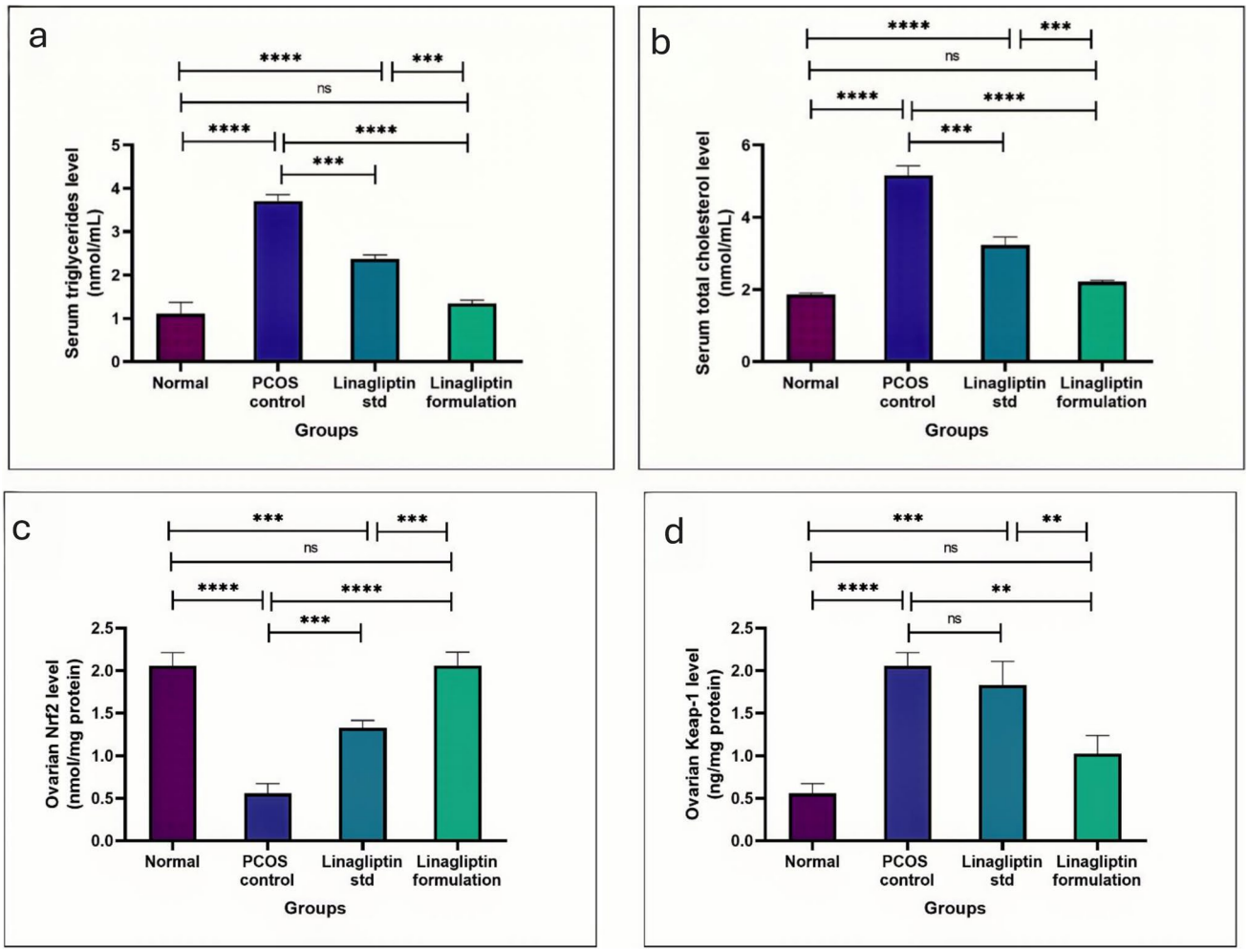

Fig. 4 Effect of linagliptin and its formulation on **a** Serum Total Triglycerides levels, **b** Cholesterol levels, **c** the Ovarian levels of nuclear factor erythroid 2-related factor 2 (Nrf2), and the Ovarian levels of nuclear factor erythroid 2-related factor 2 (Nrf2) and **d** Kelch-like ECH associated protein 1 (Keap1) in PCOS-Induced Rats. Data are presented as mean ± SEM ($n = 6$). Levels of significance include ns: non-significant, * $p<0.05$, ** $p<0.01$, *** $p<0.001$, ****$p<0.0001$

improved lipid-lowering efficacy compared to standard linagliptin solution. These findings support the therapeutic potential of linagliptin in mitigating PCOS-induced dyslipidemia and suggest that formulation optimization may further enhance its clinical utility. This observation aligns with the hypothesis that encapsulation within HA-coated liposomes enhances not only glucose regulation but also lipid metabolism. The improved lipid profile may be attributed to several interrelated mechanisms.

First, linagliptin's DPP-4 inhibitory action indirectly influences lipid metabolism through incretin-mediated pathways. Prolonged GLP-1 activity enhances hepatic lipid oxidation, reduces de novo lipogenesis, and promotes lipoprotein clearance. In PCOS and insulin-resistant states, this mechanism contributes to the correction of dyslipidemia, often characterized by elevated triglycerides and low HDL-C levels [44].

Second, the HA-coated liposomal carrier likely augmented linagliptin's tissue-specific bioavailability, particularly in the liver and adipose tissue, where CD44 receptors are expressed and metabolic regulation occurs. This targeted delivery can modulate hepatic DPP-4 expression and reduce lipid accumulation through improved insulin signaling and downregulation of inflammatory mediators involved in hepatic steatosis [78].

Additionally, the sustained-release behavior of the liposomal system may have maintained steady therapeutic levels of linagliptin, avoiding the pharmacokinetic fluctuations associated with conventional formulations. This steady DPP-4 inhibition could provide continuous metabolic modulation, translating into improved lipid parameters. The intrinsic anti-inflammatory and antioxidative effects of HA may further attenuate cytokine-induced hepatic lipid synthesis and improve systemic lipid homeostasis [27].

Taken together, these findings suggest that the HA-coated linagliptin liposomal formulation exerts a dual pharmacological benefit: improved glycemic control and concurrent amelioration of dyslipidemia. This dual effect highlights the potential of HA-based nanocarriers as multifunctional platforms capable of addressing both metabolic and inflammatory components of PCOS-associated metabolic syndrome.

It should be noted that polymeric nanoparticles such as PLGA or chitosan systems can achieve controlled release and biodegradability with lesser susceptibility to oxidation or hydrolysis compared to traditional liposomes, but may require more complex fabrication and often lack the intrinsic biocompatibility and membrane-like structure of lipid vesicles [82].

The Effect on Ovarian Levels of Nrf2 and Keap1 Levels

In the present study, ovarian Nrf2 levels were significantly reduced in the PCOS control group compared to the Normal group ($p < 0.0001$), reflecting compromised antioxidant defense mechanisms typically associated with PCOS pathophysiology. Treatment with Linagliptin in both standard and formulation forms resulted in a notable upregulation of ovarian Nrf2 levels, with the formulation group exhibiting a significantly greater increase than the standard linagliptin solution ($p < 0.001$). Although neither treatment fully restored Nrf2 levels to normal values, the Linagliptin formulation demonstrated superior efficacy, suggesting its potential for enhancing oxidative stress modulation and restoring redox balance in PCOS-afflicted ovarian tissue (Fig. 4c).

Moreover, Keap1 expression was significantly elevated in the PCOS group relative to the normal group ($p < 0.0001$), consistent with impaired Nrf2 signaling and heightened oxidative stress in PCOS pathology. Notably, there was no significant difference between the PCOS control and linagliptin standard groups, indicating limited efficacy of the standard treatment in downregulating Keap1. In contrast, the linagliptin formulation group exhibited a significant reduction in Keap1 expression compared to the standard treatment ($p < 0.01$), suggesting superior modulation of redox regulatory pathways. These results highlight the enhanced potential of the formulation in restoring antioxidant defense via Keap1-Nrf2 axis correction in PCOS (Fig. 4d).

Previous research has established that the regulation of oxidative stress is critically dependent on the Keap1/Nrf2 signaling pathway [83]. Under physiological conditions, Nrf2 is predominantly bound to its cytoplasmic inhibitor, Keap1, maintaining Nrf2 in an inactive state. In response to elevated levels of reactive oxygen species (ROS), Nrf2 dissociates from Keap1 and translocate into the nucleus, where it binds to antioxidant response elements (AREs) within the promoter regions of target genes. This interaction induces the transcription of key antioxidant enzymes, such as superoxide dismutase (SOD) and heme oxygenase-1 (HO-1), thereby enhancing the cellular antioxidant defense mechanisms [84]. The Keap1/NRF2 signaling pathway initially responds to the heightened oxidative stress characteristic of PCOS. However, chronic oxidative stress exposure, a persistent feature of the PCOS microenvironment, eventually leads to dysfunctional or exhausted antioxidant capacity, resulting in impaired Nrf2 expression and activity. This failure of the primary cytoprotective mechanism significantly contributes to the systemic and ovarian redox imbalance observed in PCOS. Consequently, the compromised Keap1/Nrf2 axis exacerbates cellular damage, particularly within the ovarian follicles and granulosa cells, which is hypothesized to be a key molecular mechanism underlying ovarian dysfunction and subfertility in women with PCOS [85]. On the other hand, linagliptin was reported as a potent activator of the Nrf2 antioxidant signaling pathway, leading to the subsequent downregulation of its cytosolic repressor, Keap1, across a spectrum of *in vitro* and *in vivo* models including vascular injury, and neurotoxicity [86, 87]. Consequently, linagliptin's therapeutic potential for PCOS is fundamentally linked to re-establishment of redox homeostasis via the Keap1/NRF2 pathway playing a pivotal role in the amelioration of core PCOS symptoms.

Encapsulation of linagliptin within HA-coated liposomes enhanced its bioavailability, stability, and tissue distribution, likely facilitating greater exposure to ovarian tissue. HA's affinity for CD44 receptors, overexpressed in inflamed ovarian environments, promotes receptor-mediated uptake, while its intrinsic antioxidant and anti-inflammatory properties synergize with linagliptin's activity. Moreover, the sustained-release profile of the liposomal system ensures continuous DPP-4 inhibition and prolonged stimulation of antioxidant signaling cascades [27, 78].

The Effect on Histopathological Examination of the Ovaries

Microscopic examination of different ovarian samples revealed the following observations. Control samples exhibited typical histological characteristics of ovarian parenchyma, including an ovarian cortical zone with growing follicles at various stages of development and maturation. These follicles showed intact oocytes and surrounding granulosa cells (Fig. 5a). Few corpora lutae, intact interstitial tissue as well as ovarian medulla. Model PCOS samples (Fig. 5b) showed significant damage of ovarian follicles' integrity with multiple figures of large cystic follicles (star) with marked degenerative changes, nuclear pyknosis and apoptotic bodies' remnants of granulosa cells with lost oocytes integrity.

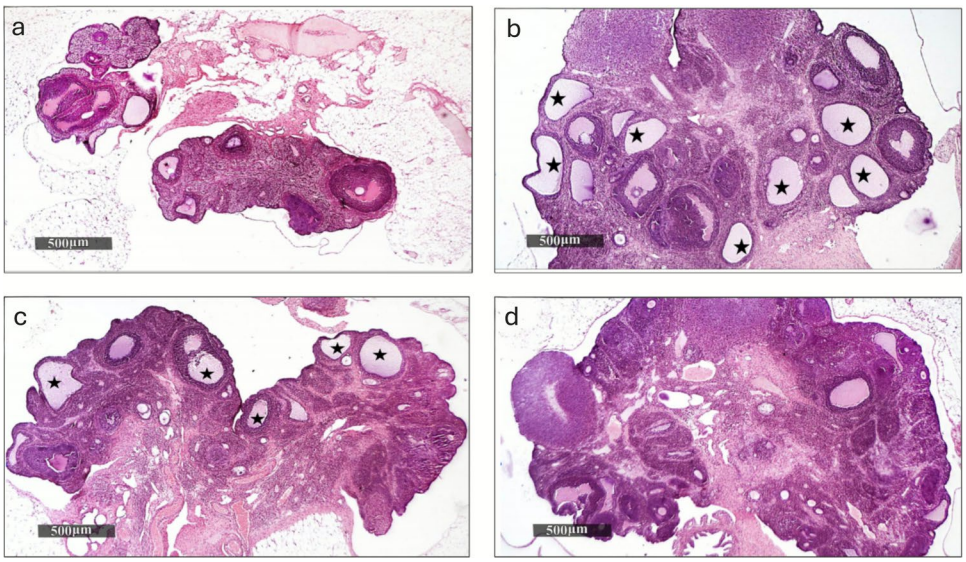

Fig. 5 Histopathological examination of ovarian tissue from all the groups **a** Normal group, **b** PCOS control group, **c** Linagliptin treated group, and **d** Linagliptin formulation treated group. The stars represent the cystic follicles

Samples of the linagliptin standard treatment (Fig. 5c) showed minimal protective efficacy with persistent records of multiple large cystic follicles (star) with degenerated granulosa cells. Samples of linagliptin formulation (Fig. 5d) showed significant reduction of ovarian cysts and degenerative changes with many viable oocytes and apparent intact morphological features of growing follicles granulosa cells and occasional apoptotic bodies figures in some follicles with intact interstitial tissue and vasculatures were demonstrated.

Conclusion

The present study successfully demonstrates the development of a targeted, hyaluronic acid-coated liposomes system for linagliptin, to enhance bioavailability and enable selective ovarian targeting for the treatment of polycystic ovary syndrome. The integration of artificial intelligence models into the formulation optimization process introduced a novel and efficient approach to predict entrapment efficiency, thereby reducing the experimental burden and enhancing the precision of formulation design, which is considered a forward-looking paradigm in pharmaceutical sciences, particularly in the development of disease-specific therapies. The current preclinical data confirm that linagliptin has a promising therapeutic potential for treating PCOS via achieving a significant amelioration of the insulin-resistant state as evidenced by nearly normalization of HOMA-IR, lipids, Nrf2 and Keap-1 levels, establishing its superior potential for clinical translation. Crucially, the optimized linagliptin formulation demonstrated a statistically marked advantage, delivering the greatest therapeutic effect across all measured metabolic and molecular parameters. Future directions should include comprehensive pharmacokinetic and biodistribution studies to confirm the targeting efficiency of the formulation, as well as long-term safety evaluations. While HA modification enhances targeting specificity, it can introduce challenges in large-scale manufacturing, including reproducibility of ligand density and consistency of surface coverage, which are critical for predictable *in-vivo* performance. Surface functionalization techniques must be tightly controlled to ensure batch-to-batch uniformity, a factor that merits further process optimization. Additionally, long-term stability, particularly under varied storage conditions, remains an inherent challenge for lipid-based carriers due to susceptibility to lipid oxidation and vesicle fusion; incorporation of stabilizing excipients or lyophilization protocols could help address this concern and should be systematically evaluated in future work. Moreover, clinical translation will require validation in larger animal models and eventually in human clinical trials. Overall, this work contributes to the growing body of evidence supporting the role of intelligent drug delivery systems and AI-driven formulation strategies in enhancing the therapeutic landscape for complex endocrine disorders such as PCOS.

Acknowledgements The authors would like to express their sincere gratitude to Professor M. Abdelrazik, Professor of Pathology, Faculty of Veterinary Medicine, Cairo University, for his valuable participation in the histopathological examination of this study.

Author Contributions Marwa H.S. Dawoud, Mai A. Zaafan contributed equally to the conception, design, execution, and analysis of this research project. Marwa H.S. Dawoud and Mai A. Zaafan shared in the final approval of the version to be published. Marwa H.S. Dawoud, Aml.H.Zaghloul, Karen.S. Zakhari, Mai.I.Mahmoud, Zeinab.M.Elnagdy, Nyera H. El-Shafei, and Mai A. Zaafan shared in

the conception or design of the work; or the acquisition, analysis, or interpretation of data for the work; and drafting the work or revising it critically for important intellectual content. Marwa H.S. Dawoud and Mai A. Zaafan shared in the final approval of the version to be published. Marwa H.S. Dawoud, Aml.H.Zaghloul, Karen.S. Zakhari, Mai.I.Mahmoud, Zeinab.M.Elnagdy, Nyera H. El-Shafei, and Mai A. Zaafan agreed to be accountable for all aspects of the work in ensuring that questions related to the accuracy or integrity of any part of the work are appropriately investigated and resolved.

Funding Open access funding provided by The Science, Technology & Innovation Funding Authority (STDF) in cooperation with The Egyptian Knowledge Bank (EKB).

Data Availability The datasets generated during and/or analyzed during the current study are available from the corresponding author on reasonable request.

Declarations

Ethics Statement The *in-vivo* study on mice was conducted in strict accordance with the ARRIVE guidelines (EU Directive 2010/63/EU for animals experiment). The study protocol was reviewed and approved by the Ethics Committee of the Faculty of Pharmacy, MSA University. All procedures involving animals were performed with the utmost care to ensure their welfare and to minimize any potential distress. (Approval number PT88/REC88/2025P).

Conflict of interests The authors declare no known competing financial interests or personal relationships that could have appeared to influence the work reported in this paper.

Disclaimer AI technology was used only in editing and language clarity.

References

1. Stener-Victorin E, Teede H, Norman RJ, Legro R, Dokras A, Laven J, et al. Polycystic ovary syndrome. Nat Rev Dis Primers. 2024;10:27.
2. Abdalla MA, Deshmukh H, Atkin S, Sathyapalan T. A review of therapeutic options for managing the metabolic aspects of polycystic ovary syndrome. Ther Adv Endocrinol Metab. 2020. https://doi.org/10.1177/2042018820938305.
3. Adam L, Adam L. Comprehensive overview of polycystic ovary syndrome: pathophysiology, clinical features, and emerging therapeutic approaches. Obes Med [Internet]. 2025 [cited 2025 Nov 8];55. https://www.sciencedirect.com/science/article/pii/S2451847625000260. Accessed 8 Nov 2025.
4. Paravati R, De Mello N, Onyido EK, Francis LW, Brüsehafer K, Younas K, et al. Differential regulation of osteopontin and CD44 correlates with infertility status in PCOS patients. J Mol Med. 2020;98:1713–25. https://doi.org/10.1007/s00109-020-01985-w.
5. Rasheed MW, Mahboob A, Amin L, Hussain A. Ranking polycystic ovarian syndrome (PCOS) drugs using degree-based indices in QSPR models and CRITIC-driven MCDM methods. Sci Rep. 2025. https://doi.org/10.1038/s41598-025-99508-5.
6. Rojas J, Chávez M, Olivar L, Rojas M, Morillo J, Mejías J, et al. Polycystic ovary syndrome, insulin resistance, and obesity: navigating the pathophysiologic labyrinth. Int J Reprod Med. 2014;2014:1–17. https://doi.org/10.1155/2014/719050.
7. Amato MC, Vesco R, Vigneri E, Ciresi A, Giordano C. Hyperinsulinism and polycystic ovary syndrome (PCOS): role of insulin clearance. J Endocrinol Invest. 2015;38:1319–26. https://doi.org/10.1007/S40618-015-0372-X.
8. Kumbhar PS, Chavan R, Darekar S, Kolekar K, Sequeira A, Vishwas S, et al. Bridging gap in treatment of polycystic ovarian syndrome through drug repurposing: what we achieved and where we are? Naunyn Schmiedebergs Arch Pharmacol. 2025;398:3213–40. https://doi.org/10.1007/S00210-024-03578-7.
9. Kabel AM, Al-Shehri AH, Al-Talhi RA, Abd Elmaaboud MA. The promising effect of linagliptin and/or indole-3-carbinol on experimentally-induced polycystic ovarian syndrome. Chem Biol Interact. 2017;273:190–9. https://doi.org/10.1016/j.cbi.2017.06.009.
10. Bednarz K, Kowalczyk K, Cwynar M, Czapla D, Czarkowski W, Kmita D, et al. The role of Glp-1 receptor agonists in insulin resistance with concomitant obesity treatment in polycystic ovary syndrome. Int J Mol Sci [Internet]. 2022 [cited 2025 Nov 8];8. https://www.mdpi.com/1422-0067/23/8/4334. Accessed 8 Nov 2025.
11. Chen X, Wan Y, Xie L. Insulin Resistance in PCOS: pathophysiological mechanisms of menstrual dysfunction and evidence-based treatment strategies. Biol Reprod [Internet]. 2025 [cited 2025 Nov 12];ioaf197. https://doi.org/10.1093/BIOLRE/IOAF197/8244406.
12. Rashid R, Mir SA, Kareem O, Ali T, Ara R, Malik A, et al. Polycystic ovarian syndrome-current pharmacotherapy and clinical implications. J Obstet Gynaecol Res [Internet]. 2022 [cited 2025 Nov 12];61:40–50. https://www.sciencedirect.com/science/article/pii/S1028455921003132. Accessed 12 Nov 2025.
13. Shah P, Chavda K, Vyas B, Patel S. Formulation development of linagliptin solid lipid nanoparticles for oral bioavailability enhancement: role of P-gp inhibition. Drug Deliv Transl Res. 2021;11:1166–85. https://doi.org/10.1007/s13346-020-00839-9.
14. Pawar K, Kamble R, Patil S. Linagliptin-loaded bilosomes for oral administration: formulation, optimization by Box-Behnken design, in-vitro, and in-vivo assessment. J Drug Deliv Sci Technol [Internet]. 2025 [cited 2025 Nov 10];108:106879. https://www.sciencedirect.com/science/article/pii/S1773224725002825. Accessed 10 Nov 2025.
15. Bhikshapathi DVRN, Gadi Raju RLR. Enhancement of solubility and bioavailability of linagliptin solid dispersions by solvent evaporation technique with novel carriers. Pharmacy 2016 [conference abstract]; 2016 Jul 14–15; Philadelphia. Available from: https://www.scitechnol.com/proceedings/enhancement-of-solubility-and-bioavailability-of-linagliptin-solid-dispersions-by-solventevaporation-technique-with-nov-441.html.
16. Szafraniec-Szczęsny J, Antosik-Rogóż A, Knapik-Kowalczuk J, Kurek M, Szefer E, Gawlak K, et al. Compression-induced phase transitions of bicalutamide. Pharmaceutics. 2020. https://doi.org/10.3390/pharmaceutics12050438.
17. Sweed NM, Elbalkiny HT, Magdy E, Ramadan M, Mahmoud S, Mohamed T, et al. Optimization of Linagliptin-loaded polymersomes via response surface methodology: A repurposed therapeutic strategy for hepatic encephalopathy prevention. J Drug Deliv Sci Technol [Internet]. 2025 [cited 2025 Oct 26];108. https://

www.sciencedirect.com/science/article/pii/S177322472500258. Accessed 26 Oct 2025.
18. Nirwan N, Anjaneyulu YP, Sultana Y, Vohora D. Development of linagliptin-loaded liposomes using aspartic acid conjugate for bone-targeted delivery to combat osteoporosis. J Drug Target. 2025;33:1014–25. https://doi.org/10.1080/1061186X.2025.2467089.
19. Kamaly N, Yameen B, Wu J, Farokhzad OC. Degradable controlled-release polymers and polymeric nanoparticles: mechanisms of controlling drug release. Chem Rev. 2016. https://doi.org/10.1021/acs.chemrev.5b00346.
20. El-Samaligy MS, Afifi NN, Mahmoud EA. Evaluation of hybrid liposomes-encapsulated silymarin regarding physical stability and in vivo performance. Int J Pharm. 2006;319:121–9.
21. Lasic D. Liposomes: Synthetic lipid microspheres serve as multipurpose vesicles for the delivery of drugs, genetic material and cosmetics. Am Scientist [Internet]. 1992 [cited 2015 Nov 19];80:250–7. https://scholar.google.com.eg/scholar?q=liposomes%2C+synthetic+lipid+microspheres+serve+as+multipurpose+vesicles&btnG=&hl=en&as_sdt=0%2C5#0. Accessed 19 Nov 2015.
22. Sweed NM, Zaafan MA, El-Bishbishy MH, Dawoud MHS. The pulmonary protective potential of vanillic acid-loaded TPGS-liposomes: modulation of miR-217/MAPK/NF-κb signalling pathway. J Microencapsul. 2024;41:255–68.
23. Nsairat H, Khater D, Sayed U, Odeh F, Al Bawab A, Alshaer W. Liposomes: structure, composition, types, and clinical applications. Heliyon. 2022. https://doi.org/10.1016/j.heliyon.2022.e09394.
24. Khan AA, Allemailem KS, Almatroodi SA, Almatroudi A, Rahmani AH. Recent strategies towards the surface modification of liposomes: an innovative approach for different clinical applications. 3 Biotech. 2020. https://doi.org/10.1007/s13205-020-2144-3.
25. Knopf-Marques H, Pravda M, Wolfova L, Velebny V, Schaaf P, Engin Vrana N, et al. Hyaluronic acid and its derivatives in coating and delivery systems: applications in tissue engineering, regenerative medicine and immunomodulation. Adv Healthc Mater. 2016;5:2841–55. https://doi.org/10.1002/ADHM.201600316.
26. How KN, Yap WH, Lim CLH, Goh BH, Lai ZW. Hyaluronic acid-mediated drug delivery system targeting for inflammatory skin diseases: a mini review. Front Pharmacol. 2020. https://doi.org/10.3389/fphar.2020.01105.
27. Kuna SK, Choppala AD. Biocompatible osimertinib nanoliposomes coated with PEGylated hyaluronic acid enhanced tumor selectivity and cytotoxicity via CD44-mediated NSCLC targeting: development, characterization and in-vitro biochemical studies. J Appl Pharm Sci. 2023;13:204–13.
28. Ni C, Zhang Z, Wang Y, Zhang Z, Guo X, Lv H. Hyaluronic acid and HA-modified cationic liposomes for promoting skin penetration and retention. J Control Release. 2023;357:432–43. https://doi.org/10.1016/j.jconrel.2023.03.049.
29. Schwalbe N, Wahl B. Artificial intelligence and the future of global health. Lancet. 2020;395:1579–86.
30. Serrano DR, Luciano FC, Anaya BJ, Ongoren B, Kara A, Molina G, et al. Artificial intelligence (AI) applications in drug discovery and drug delivery: revolutionizing personalized medicine. Pharmaceutics. 2024. https://doi.org/10.3390/pharmaceutics16101328. (**Multidisciplinary Digital Publishing Institute (MDPI)**).
31. Dey H, Arya N, Mathur H, Chatterjee N, Jadon R. Exploring the Role of Artificial Intelligence and Machine Learning in Pharmaceutical Formulation Design. Int J Newgen Res Pharm Healthcare. 2024;30–41.https://doi.org/10.61554/ijnrph.v2i1.2024.67. Lloyd Institute of Management and Technology.
32. Bolikulov F, Nasimov R, Rashidov A, Akhmedov F, Cho YI. Effective methods of categorical data encoding for artificial intelligence algorithms. Mathematics. 2024. https://doi.org/10.3390/math12162553.
33. Dawoud MHS, Fayez AM, Mohamed RA, Sweed NM. Optimization of nanovesicular carriers of a poorly soluble drug using factorial design methodology and artificial neural network by applying quality by design approach. Pharm Dev Technol. 2021;0:1–50. https://doi.org/10.1080/10837450.2021.1980009.
34. Dawoud MHS, Mannaa IS, Abdel-Daim A, Sweed NM. Integrating artificial intelligence with quality by design in the formulation of lecithin/chitosan nanoparticles of a poorly water-soluble drug. AAPS PharmSciTech. 2023;24:169. https://doi.org/10.1208/s12249-023-02609-5.
35. Arpicco S, Lerda C, Dalla Pozza E, Costanzo C, Tsapis N, Stella B, et al. Hyaluronic acid-coated liposomes for active targeting of gemcitabine. Eur J Pharm Biopharm. 2013;85:373–80. https://doi.org/10.1016/J.EJPB.2013.06.003.
36. Qhattal HSS, Hye T, Alali A, Liu X. Hyaluronan polymer length, grafting density, and surface poly(ethylene glycol) coating influence in vivo circulation and tumor targeting of hyaluronan-grafted liposomes. ACS Nano. 2014;8:5423–40. https://doi.org/10.1021/nn405839n.
37. Johnston MJW, Edwards K, Karlsson G, Cullis PR. Influence of drug-to-lipid ratio on drug release properties and liposome integrity in liposomal doxorubicin formulations. J Liposome Res. 2008;18:145–57. https://doi.org/10.1080/08982100802129372.
38. Goos P, Jones B, Syafitri U. I-optimal design of mixture experiments. J Am Stat Assoc. 2016. https://doi.org/10.1080/01621459.2015.1136632.
39. Hassan OF, Dawoud MHS, Ibrahim SM. Selenium and iron oxide nanoparticles mitigate doxorubicin-induced cardiomyopathy in rats via Nox1/p53 pathway inhibition. J Pharm Pharmacol. 2025. https://doi.org/10.1093/jpp/rgaf079.
40. Dawoud MHS, Abdel-Daim A, Nour MS, Sweed NM. A quality by design paradigm for albumin-based nanoparticles: formulation optimization and enhancement of the antitumor activity. J Pharm Innov. 2023. https://doi.org/10.1007/s12247-022-09698-y.
41. Sweed NM, Dawoud MHS, Aborehab NM, Ezzat SM. An approach for an enhanced anticancer activity of ferulic acid-loaded polymeric micelles via MicroRNA-221 mediated activation of TP53INP1 in caco-2 cell line. Sci Rep. 2024. https://doi.org/10.1038/s41598-024-52143-y.
42. Dawoud MHS, Elbalkiny HT, Gharib YEM, Fakkar SAA, Saber R, Yanni ME, et al. Beyond erectile dysfunction: optimization of vardenafil dihydrochloride for hepatic encephalopathy prophylaxis using hybrid lipid polymeric nanoparticles formulation. J Drug Deliv Sci Technol. 2025. https://doi.org/10.1016/j.jddst.2025.106787.
43. Dandekar, Dandekar, Manoj P., Manasi Tadas, Srilakshmi Satthi, Aditi Jangli, et al. Oxyberberine revokes letrozole-induced polycystic ovarian syndrome and depression-like behavior in female Sprague-Dawley rats. Eur J Pharmacol [Internet]. 2025 [cited 2025 Nov 10];997:177613. https://www.sciencedirect.com/science/article/pii/S001429992500367X. Accessed 10 Nov 2025.
44. Folasade Omobolanle A, Oluwatobi Olayiwola Y, Damilola Ayodeji B, Marcus Olaoye I, Mariam Olayinka A, George Adetomiwa E. Linagliptin Efficacy on Hyperglycemia, Oxidative Stress, and Inflammation in Gestational Diabetes Mellitus. Clin J Obstet Gynecol. Heighten Science Publications Corporation: 2024;7:093–9. https://doi.org/10.29328/journal.cjog.1001171.
45. Antunes, Luciana C., Jessica L. Elkfury, Manoela N. Jornada, Kelly C. Foletto, Marcello C. Bertoluci. Validation of HOMA-IR in a model of insulin-resistance induced by a high-fat diet in Wistar rats. Arch Endocrinol Metab [Internet]. 2016 [cited 2025 Nov 10];60:138–42. https://www.scielo.br/j/aem/a/h4B3P8qNqYnRvL5vGT6rgSj/?format=html&lang=en. Accessed 10 Nov 2025

46. Culling C. Handbook of histopathological and histochemical techniques: including museum techniques [Internet]. 2013 [cited 2024 Dec 8]. https://books.google.com/books?hl=en&lr=&id=HhTBAAAQBAJ&oi=fnd&pg=PP1&dq=Handbook+of+histopathological+and+histochemical+techniques:+including+museum+techniques&ots=0IvacRMvHP&sig=6amHsgzsrl_iXeELN0ii9JBnEas. Accessed 8 Dec 2024.
47. Song C, Ristenpart T, Shmatikov V. Machine learning models that remember too much. Proceedings of the ACM Conference on Computer and Communications Security. Association for Computing Machinery; 2017. pp. 587–601. https://doi.org/10.1145/3133956.3134077.
48. Maleki F, Ovens K, Gupta R, Reinhold C, Spatz A, Forghani R. Generalizability of machine learning models: quantitative evaluation of three methodological pitfalls. Radiology: Artificial Intelligence. 2023. https://doi.org/10.1148/ryai.220028.
49. Politis SN, Colombo P, Colombo G, Rekkas DM. Design of experiments (DoE) in pharmaceutical development. Drug Dev Ind Pharm. 2017. https://doi.org/10.1080/03639045.2017.1291672.
50. Thabet Y, Elsabahy M, Eissa NG. Methods for preparation of niosomes: a focus on thin-film hydration method. Methods. 2022;199:9–15. https://doi.org/10.1016/j.ymeth.2021.05.004.
51. Marinho A, Nunes C, Reis S. Hyaluronic acid: a key ingredient in the therapy of inflammation. Biomolecules. 2021. https://doi.org/10.3390/biom11101518.
52. Ravar F, Saadat E, Gholami M, Dehghankelishadi P, Mahdavi M, Azami S, et al. Hyaluronic acid-coated liposomes for targeted delivery of paclitaxel, in-vitro characterization and in-vivo evaluation. J Control Release. 2016;229:10–22. https://doi.org/10.1016/j.jconrel.2016.03.012.
53. Longmire M, Choyke PL, Kobayashi H. Clearance properties of nano-sized particles and molecules as imaging agents: considerations and caveats. Nanomedicine. 2008. https://doi.org/10.2217/17435889.3.5.703.
54. Kari OK, Tavakoli S, Parkkila P, Baan S, Savolainen R, Ruoslahti T, et al. Light-activated liposomes coated with hyaluronic acid as a potential drug delivery system. Pharmaceutics MDPI AG. 2020;12:1–24. https://doi.org/10.3390/pharmaceutics12080763.
55. Liu J, Wang F, Luo F. The role of JAK/STAT pathway in fibrotic diseases: molecular and cellular mechanisms. Biomolecules. 2023. https://doi.org/10.3390/biom13010119.
56. Blech S, Ludwig-Schwellinger E, Gräfe-Mody EU, Withopf B, Wagner K. The metabolism and disposition of the oral dipeptidyl peptidase-4 inhibitor, linagliptin, in humans. Drug Metab Dispos. 2010;38:667–78. https://doi.org/10.1124/dmd.109.031476.
57. Le HV, Le Cerf D. Colloidal polyelectrolyte complexes from hyaluronic acid: preparation and biomedical applications. Small. 2022. https://doi.org/10.1002/smll.202204283.
58. Torchilin V. Recent advances with liposomes as pharmaceutical carriers. Nat Rev Drug Discov [Internet]. 2005 [cited 2014 Jun 26];4:145–60. http://www.nature.com/nrd/journal/v4/n2/abs/nrd1632.html. Accessed 26 Jun 2014.
59. Hagquist C, Stenbeck M. Goodness of fit in regression analysis-R 2 and G 2 reconsidered. Qual Quant. 1998. https://doi.org/10.1023/a:1004328601205.
60. Rigg J, Hankins M. Reducing and quantifying over-fitting in regression models. Value Health. 2015;18:A5. https://doi.org/10.1016/j.jval.2015.03.027.
61. Ehresman J, Lubelski D, Pennington Z, Hung B, Ahmed AK, Azad TD, et al. Utility of prediction model score: a proposed tool to standardize the performance and generalizability of clinical predictive models based on systematic review. J Neurosurg Spine. 2021;34:779–87. https://doi.org/10.3171/2020.8.SPINE20963.
62. Noshi SH, Dawoud MHS, Ibrahim MS. A quality by design approach for the optimization of olmesartan medoxomil-orodispersible lyophilisates: in vitro/in vivo evaluation. J Appl Pharm Sci. 2022;12:175–85. https://doi.org/10.7324/JAPS.2022.120617.
63. Renaud O, Victoria-Feser MP. A robust coefficient of determination for regression. J Stat Plan Inference. 2010;140(7):1852–62. https://doi.org/10.1016/j.jspi.2010.01.008.
64. Danaei M, Dehghankhold M, Ataei S, Hasanzadeh Davarani F, Javanmard R, Dokhani A, et al. Impact of particle size and polydispersity index on the clinical applications of lipidic nanocarrier systems. Pharmaceutics. 2018. https://doi.org/10.3390/pharmaceutics10020057.
65. Cheng L, Zhang M, Dong L, Wang Y, Dong J, Wu F, et al. Interaction between hyaluronic acid and phospholipid bilayer and its influence on stability and bioavailability of luteolin-loaded liposomes. Food Chem X. 2025. https://doi.org/10.1016/j.fochx.2025.103116.
66. Malkawi A, Alrabadi N, Kennedy RA. Dual-acting zeta-potential-changing micelles for optimal mucus diffusion and enhanced cellular uptake after oral delivery. Pharmaceutics. 2021. https://doi.org/10.3390/pharmaceutics13070974.
67. Cao FH, OuYang WQ, Wang YP, Yue PF, Li SP. A combination of a microemulsion and a phospholipid complex for topical delivery of oxymatrine. Arch Pharm Res. 2011;34:551–62. https://doi.org/10.1007/s12272-011-0405-8.
68. Hammad RW, Sanad RAB, Abdelmalak NS, Latif R. Cubosomal functionalized block copolymer platform for dual delivery of linagliptin and empagliflozin: recent advances in synergistic strategies for maximizing control of high-risk type II diabetes. Drug Deliv Transl Res. 2024;14:678–95.
69. Hussein HA, Abdullah MA. Novel drug delivery systems based on silver nanoparticles, hyaluronic acid, lipid nanoparticles and liposomes for cancer treatment. Appl Nanosci. 2022. https://doi.org/10.1007/s13204-021-02018-9.
70. Abbas A, Eissa NG, El-Bassossy HM, Ghorab MM, El Nahas HM. Polymeric linagliptin nanoparticles as a sustained release treatment for type 2 diabetes. J Drug Deliv Sci Technol. 2024;93:105438. https://doi.org/10.1016/j.jddst.2024.105438.
71. Bonechi C, Tamasi G, Donati A, Leone G, Consumi M, Cangeloni L, et al. Physicochemical characterization of hyaluronic acid and chitosan liposome coatings. Appl Sci. 2021. https://doi.org/10.3390/app112412071.
72. Akbarzadeh A, Rezaei-Sadabady R, Davaran S, Joo SW, Zarghami N, Hanifehpour Y, et al. Liposome: classification, preparation, and applications. Nanoscale Res Lett. 2013. https://doi.org/10.1186/1556-276X-8-102.
73. Polomska A, Leroux JC, Brambilla D, Wiley-VCH Verlag. Layer-by-layer coating of solid drug cores: a versatile method to improve stability, control release and tune surface properties. Macromol Biosci. 2017. https://doi.org/10.1002/mabi.201600228.
74. Kumar KK, Sharma PK, Srinivas L. Development of agglomerated crystals of olmesartan medoxomil by spherical crystalization technique for enhancing the micromeritic and solubility property. World J Pharm Res. 2016;5:646–75.
75. Shah H, Mahajan SR. Screening of topical gel containing lycopene and dexamethasone against UV radiation induced photoaging in mice. Biomed Aging Pathol. 2014;4:303–8.
76. John J (2026) Advancements in nano-based drug delivery systems for therapeutics: a comprehensive review. RSC Pharmaceutics. Royal Society of Chemistry (RSC). https://doi.org/10.1039/d5pm00179j
77. Binaymotlagh R, Hajareh Haghighi F, Chronopoulou L, Palocci C. Liposome–hydrogel composites for controlled drug delivery applications. Gels. 2024. https://doi.org/10.3390/gels10040284.
78. Suksiriworapong J, Pongprasert N, Bunsupa S, Taresco V, Crucitti VC, Janurai T, et al. CD44-targeted lipid polymer hybrid nanoparticles enhance anti-breast cancer effect of *Cordyceps militaris*

extracts. Pharmaceutics. 2023. https://doi.org/10.3390/pharmaceutics15061771.
79. Sun Y, Shen X, Yang J, Tan C. Hyaluronic acid-coated nanoliposomes as delivery systems for fisetin: stability, membrane fluidity, and bioavailability. Foods. 2024. https://doi.org/10.3390/foods13152406.
80. Salari N, Mansouri K, Valipour E, Abam F, Jaymand M, Rasoulpoor S, et al. Hyaluronic acid-based drug nanocarriers as a novel drug delivery system for cancer chemotherapy: a systematic review. DARU J Pharm Sci. 2021. https://doi.org/10.1007/s40199-021-00416-6.
81. Yamamoto F, Ikeda R, Ochiai K, Hirase T, Hayashi N, et al. Long-Term Safety and Effectiveness of Linagliptin in Japanese Patients with Type 2 Diabetes and Renal Dysfunction: a Post-Marketing Surveillance Study. Diabetes Therapy [Internet]. 2020;11:523–33. https://doi.org/10.6084/m9.figshare.11418123.
82. Yusuf A, Almotairy ARZ, Henidi H, Alshehri OY, Aldughaim MS, MDPI. Nanoparticles as drug delivery systems: a review of the implication of nanoparticles' physicochemical properties on responses in biological systems. Polymers (Basel). 2023. https://doi.org/10.3390/polym15071596.
83. Sykiotis GP. Keap1/Nrf2 signaling pathway. Antioxidants [Internet]. 2021 [cited 2025 Nov 9];10:828. https://www.mdpi.com/2076-3921/10/6/828. Accessed 9 Nov 2025
84. Bellezza I, Giambanco I, Minelli A, Donato R, Elsevier B.V. Nrf2-Keap1 signaling in oxidative and reductive stress. Biochimica et Biophysica Acta (BBA) - Mol Cell Res. 2018. https://doi.org/10.1016/j.bbamcr.2018.02.010.
85. Wang Y, Li N, Zeng Z, Tang L, Zhao S, Zhou F, et al. Humanin regulates oxidative stress in the ovaries of polycystic ovary syndrome patients via the Keap1/Nrf2 pathway. Mol Hum Reprod. 2021. https://doi.org/10.1093/molehr/gaaa081.
86. Arab HH, Eid AH, Alsufyani SE, Ashour AM, El-Sheikh AAK, Darwish HW, et al. Neuroprotective impact of linagliptin against cadmium-induced cognitive impairment and neuropathological aberrations: targeting SIRT1/Nrf2 axis, apoptosis, and autophagy. Pharmaceuticals. 2023. https://doi.org/10.3390/ph16081065.
87. Nady ME, El-Raouf OMA, El-Sayed ESM. Linagliptin ameliorates tacrolimus-induced renal injury: role of Nrf2/HO-1 and HIF-1α/CTGF/PAI-1. Mol Biol Rep. 2024. https://doi.org/10.1007/s11033-024-09533-2.